

Thesis summary

From grains to rocks: the evolution of hydraulic and mechanical properties during diagenesis.

Introduction

Most of our understanding about the relationship between microstructural geometries and bulk properties arises from detailed experimental work using natural materials. However, because it is extremely rare to find natural rock formations that show variability in one microstructural attribute whilst others remain constant (as is the case for Fontainebleau sandstone which occurs over a large range of porosity values) and because the high degree of variability of rock in both time and space limit consistency and reproducibility in laboratory experiments, the testing of synthetic rock materials has become a major topic of research in the past decades. It is now well established that synthetic rocks can offer the opportunity to realistically model real rock behaviour and the evolution of effective properties throughout geological processes such as diagenesis.

The thesis entitled *From grains to rocks: evolution of hydraulic and mechanical properties during diagenesis* seeks to build upon previous theoretical and experimental studies and explore how the use of synthetic rocks prepared by sintering glass beads may help define a comprehensive framework for the influence of porosity and grain size distribution on the hydraulic and mechanical properties of crustal rocks. Although there exist a great number of other microstructural attributes which require careful deconvolved study, as they contribute to building the complex and highly variable hydromechanical behaviour of rocks that form the Earth's crust, I chose to lay the foundations of using sintered glass beads samples for rock mechanics laboratory experiments and investigate the simplest case of a two-phase (solid and gas) granular medium with no cement. Therefore, the thesis mainly focuses on the control of porosity and grain size distribution, which also stand out as first order controls of the hydromechanical properties. Ultimately, this research aims to help understanding how effective properties are derived mathematically using the rock microstructure information and constituent properties, as it is of great interest to numerous environmental and industrial applications. Indeed, the data acquired in this research should allow to improve model predictions, routinely used in many aspects of geoscience and engineering while still only relying on simple-to-measure microstructural metrics. For example, understanding how physical properties evolve during the granular densification process will help us to better understand fluid pressurisation that can lead to fracturing, a major issue for exploration drilling and thus for the management and optimisation of hydrocarbons and geothermal reservoirs.

In detail, this thesis seeks to address the following questions:

1. Can synthetic rocks made by sintering glass beads satisfactorily simulate the hydromechanical behaviour of porous crustal rocks and therefore be used to unravel the contribution of specific microstructural attributes on bulk hydromechanical properties?
2. All else being equal, what if the effect of total porosity/mean grain size variations on the onset of inelastic compaction?
3. How do the width and shape of the grain size distribution influence the mechanical behaviour and failure mode of porous granular rocks?

In order to answer the previous questions, the thesis was conducted as a systematic study of variations in physical properties, such as permeability, elastic wave velocity and strength, as a result of controlled variations in porosity or in grain size distribution. The thesis manuscript is built upon two milestones: (1) the simplest case of a two-phase granular medium with a very closely clustered grain size distribution and (2) a more complicated case where the granular medium presents a variably polydisperse grain size distribution. Beforehand, Chapter 2 of the thesis details the technique for the preparation of the synthetic rocks by viscous sintering, using a monodisperse grain size distribution or a polydisperse grain distribution, and Chapter 3 summarises the main experimental methods used to conduct the work. The following chapters introduce the results. Chapter 4 investigates how the mechanical behaviour and failure mode of monodisperse granular rocks evolve as a result of variations in porosity or in mean grain size, in both cases whilst all other microstructural geometries are kept unchanged. The mechanical data are analysed alongside microstructural data obtained using Scanning Electron Microscopy (SEM). The results and discussion are presented in: Carbillet, L., Heap, M. J., Baud, P., Wadsworth, F.B., & Reuschlé, T. (2021). Mechanical Compaction of Crustal Analogs Made of Sintered Glass Beads: The Influence of Porosity and Grain Size. *Journal of Geophysical Research: Solid Earth*, 126, e2020JB021321. <https://doi.org/10.1029/2020JB021321>. Chapter 5 addresses the influence of the degree of polydispersivity and modality of the grain size distribution on the mechanical behaviour and failure mode of porous rocks, by means of triaxial compression experiments and microstructural observations. The results and discussion have been published in: Carbillet, L., Heap, M. J., Baud, P., Wadsworth, F. B., & Reuschlé, T. (2022). The influence of grain size distribution on mechanical compaction and compaction localization in porous rocks. *Journal of Geophysical Research: Solid Earth*, 127, e2022JB025216. <https://doi.org/10.1029/2022JB025216>. Finally, Chapter 6 of the thesis gathers and puts the conclusions of the preceding chapters into perspective.

In the following, the research questions previously presented are discussed using the main results of the thesis.

Preparation of the synthetic rocks

The work conducted in this thesis relied on the preparation of synthetic rocks with variable microstructural attributes (e.g., porosity and grain size) by sintering glass beads. Sintering consists in the combination of individual discrete particles into a unique continuous body under forces acting on the particles either internally or externally. In the case where the particles that amalgamate are in a liquid state, the process is referred to as *viscous sintering*. When heated to a temperature higher than the upper temperature of the glass transition, silicate glass beads act as viscous droplets and undergo time-dependent coalescence. The viscous sintering of glass beads, similar to sediments diagenesis, results in a granular densification accompanied by a progressive decrease in porosity. Besides this, viscous sintering is also accompanied by a decrease in the connectivity of the pore space due to progressive pore shrinking, ultimately leading to pore-space isolation at a total porosity of approximately 0.03. For this research, the theoretical framework for viscous sintering was used as a guide to design samples with pre-determined microstructural attributes and to parameterise specifically for the study of chosen parameters in isolation, i.e., to vary one parameter while keeping the others constant. The thesis' originality lays in the preparation of

samples that span a wide range of porosity and grain size, which required to perfect the procedures reported in the literature, but also in the development of a new methodology for preparing samples individually.

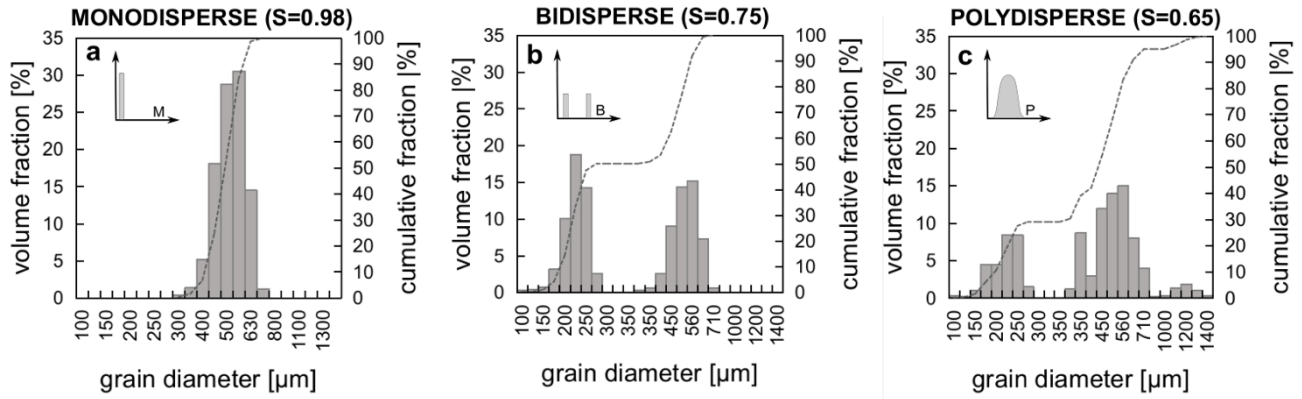


Figure 1 Types of grain size distributions used to prepare the synthetic samples used for the research. The simplest distribution which can be prepared is **(a)** a monomodal closely clustered distribution of bead sizes, which are referred to as monodisperse for simplicity. **(b)** Beads of two sizes can be mixed to prepare bidisperse distributions and **(c)** beads of various sizes can be mixed to prepare polydisperse distributions.

Practically speaking, the procedure to prepare sintered glass beads samples was structured by three main stages: the design of the grain size distribution at room temperature, the decrease of porosity up to the desired value by viscous sintering at high temperature, the sample preparation at room temperature. Figure 1 gives an overview of the type of distribution which were prepared in the course of this work: monomodal and closely clustered for the distributions referred to as monodisperse, with two principal peaks (i.e., two sizes) for the bidisperse distributions and with multiple peaks (i.e., multiple sizes) for the polydisperse distributions. S quantifies the degree of dispersivity ($0 < S < 1$, with $S = 1$ the monodisperse limit) of a distribution.

Using these distributions, synthetic rocks with porosity in the range 0.03 – 0.38 and mean grain radius between 261 and 601 μm were prepared. A collection of cylindrical samples with different porosity and grain size distribution is presented in Figure 2, alongside samples of Fontainebleau and Bentheim sandstones, two well-sorted monomineralic natural sandstones.

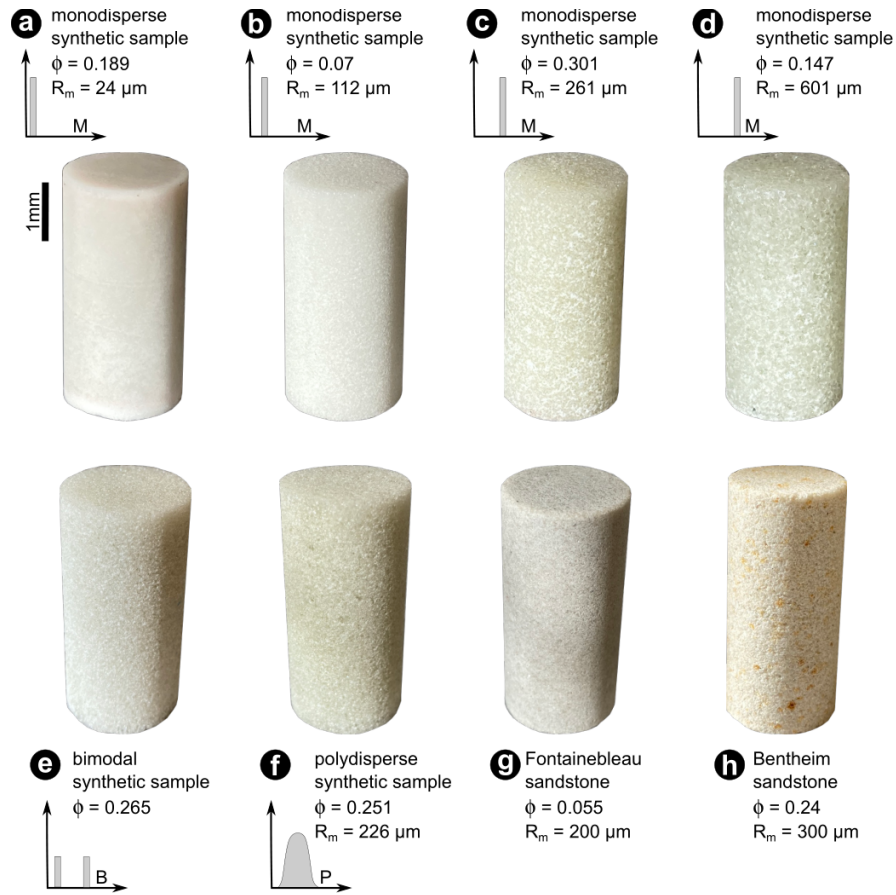


Figure 2 Overview of synthetic and natural sandstone samples with various grain size distributions. Four monodisperse distributions of grain size were used to prepare synthetic samples with mean grain radius of **(a)** 24 μm , **(b)** 112 μm , **(c)** 261 μm and **(d)** 601 μm . Glass beads from different size ranges were mixed in various proportions to prepare samples, with either **(e)** bidisperse or **(f)** polydisperse grain size distributions. The synthetic samples are presented next to two well-sorted natural sandstones which have been extensively studied in the laboratory: **(g)** a Fontainebleau sandstone sample with a porosity of 0.055 and a mean grain radius of 220 μm and **(h)** a Bentheim sandstone sample with a porosity of 0.24 and a mean grain radius of 300 μm .

Insights into the microstructure of intact synthetic samples were gained using polished thin sections observed under a scanning electron microscope (SEM). Figure 3 shows the microstructure of synthetic samples with different porosity and grain size distributions. As porosity decreases, the microstructural transition from a granular state to a non-granular state can be observed. At high porosity (Figure 3(a)(c)), adjacent beads are connected by a neck and pore space remains between the bonded grains. While a material is only truly granular when the individual grains can move relative to one another (which is the case for the glass beads prior to sintering), the high-porosity synthetic rocks are close to that granular end member case. At intermediate porosity (Figure 3(d)), sintering has progressed and begun to close the pore network. Finally, at low-porosity (Figure 3(b)), synthetic rocks exhibit pore structures close to isolated pores in a glass medium.

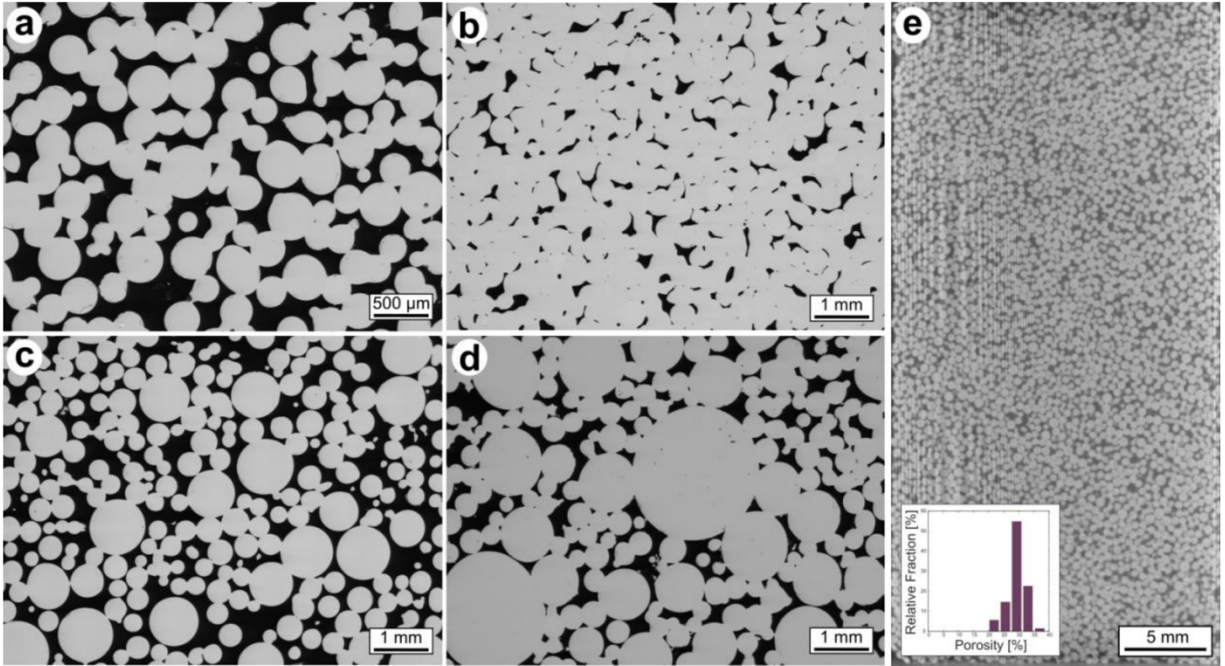


Figure 3 Microstructure of sintered glass bead samples. SEM images of monodisperse synthetic samples with a mean grain radius of 112 μm and porosity of (a) 0.32 and (b) 0.07, a (c) bidisperse synthetic sample with a porosity of 0.35 and beads with radii of 261 and 112 μm and (d) polydisperse synthetic sample with a porosity of 0.25 and mean grain radius of 454 μm . (e) 2D slice through a 3D X-ray tomography scan of a monodisperse sample with a porosity of 0.30 and a mean grain diameter of 261 μm , for which 2D porosity measurements made in a squared window of 2mm of edge length (REV) yielded values clustering around 0.30.

The use of viscous sintering allowed for pre-determining and controlling microstructural attributes such as the grain and pore size distributions and the porosity of the rock samples. Two preparation protocols were developed: the sintering of bead packs in the form of blocks from which samples were cored and the sintering of bead packs directly shaped into cylindrical samples. Ultimately, this approach allowed for the preparation of highly reproducible precisely controlled rock analogues and to parameterise specifically for the importance of porosity and grain or pore size on the mechanical behaviour of porous materials in general, thus to move beyond phenomenological approaches to naturally variable materials. Before serving as materials for deformation experiments, the synthetic samples were characterised in the laboratory and their physical properties (permeability, P- and S-waves velocity, electrical conductivity, thermal conductivity) compared to that of natural sandstones, to evaluate the suitability of sintered glass beads samples as analogues for porous sandstones.

Suitability of sintered glass beads as analogues for porous crustal rocks

Chapter 3 of the thesis provides a large dataset of petrophysical properties for the sintered glass beads samples: porosity, specific surface, P- and S-wave velocities, thermal conductivity, electrical conductivity, gas-permeability and uniaxial compressive strength. Comparing these data to those reported for the monomineralic very-well sorted Fontainebleau sandstone (which was extensively studied due to its

occurrence over a large range of porosity while other microstructural attributes remain almost constant), Chapter 3 highlighted first of all the excellent agreement between the trends in elastic wave velocities, formation factor and permeability as a function of porosity (Figure 4) for Fontainebleau sandstone, which has a mean grain radius of approximately 125 μm , and those for monodisperse synthetic samples with a mean grain size of 112 μm .

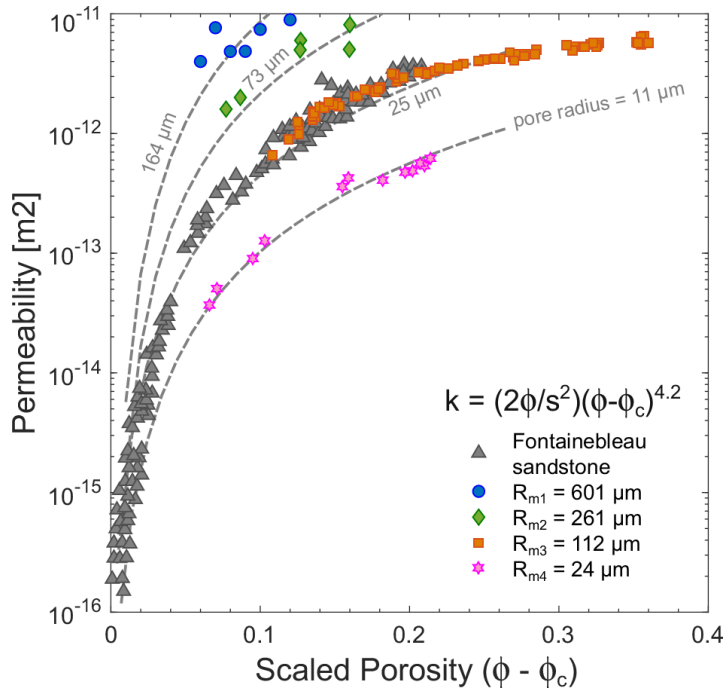


Figure 4 Permeability evolution with porosity for monodisperse synthetic samples with mean grain radius of 601 (blue circles), 261 (green diamonds), 112 (orange squares) and 24 (pink stars) μm and Fontainebleau sandstone samples (grey triangles). Grey dashed lines are model predictions for the porosity-permeability curves.

Further, using the P- and S-wave velocity in quartz and air in the Raymer-Hunt-Gardner equation (Figure 5), the thermal conductivity of silica glass in the Rayleigh-Maxwell equation, and the equivalent channel model to relate the permeability to the formation factor, the experimental datasets for sintered glass beads could be very well modelled.

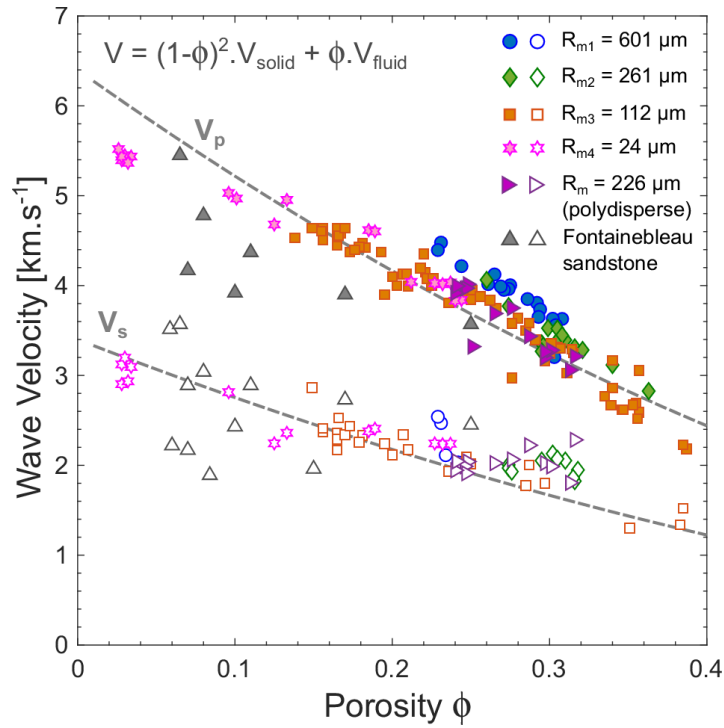


Figure 5 Porosity dependency of P- (solid symbols) and S-wave (open symbols) velocity in monodisperse synthetic samples with a mean grain radius of 601 (blue circles), 261 (green diamonds), 112 (orange squares) and 24 (pink stars), polydisperse synthetic samples (degree of polydispersivity $S = 0.89$) with a mean grain radius of 226 μm (purple right triangles) and Fontainebleau sandstone samples (grey triangles). Grey dashed lines are modelled porosity-velocity curves for V_p and V_s.

Such consistency in the transport properties of the synthetic samples with that of natural sandstones and with petrological laws validated against natural rocks, demonstrate that sintered glass bead samples can be used to accurately replicate the microstructural geometries of porous natural rocks.

The research presented in this thesis was also built upon deformation experiments performed under various stress states: uniaxial, triaxial and hydrostatic compression. The results obtained were compared to mechanical data for natural sandstones to assess the suitability of sintered glass beads to replicate the mechanical behaviour of porous crustal rocks. Figure 6 presents selected representative mechanical and microstructural data for monodisperse synthetic samples compared to data for natural samples, in particular Bentheim sandstone.

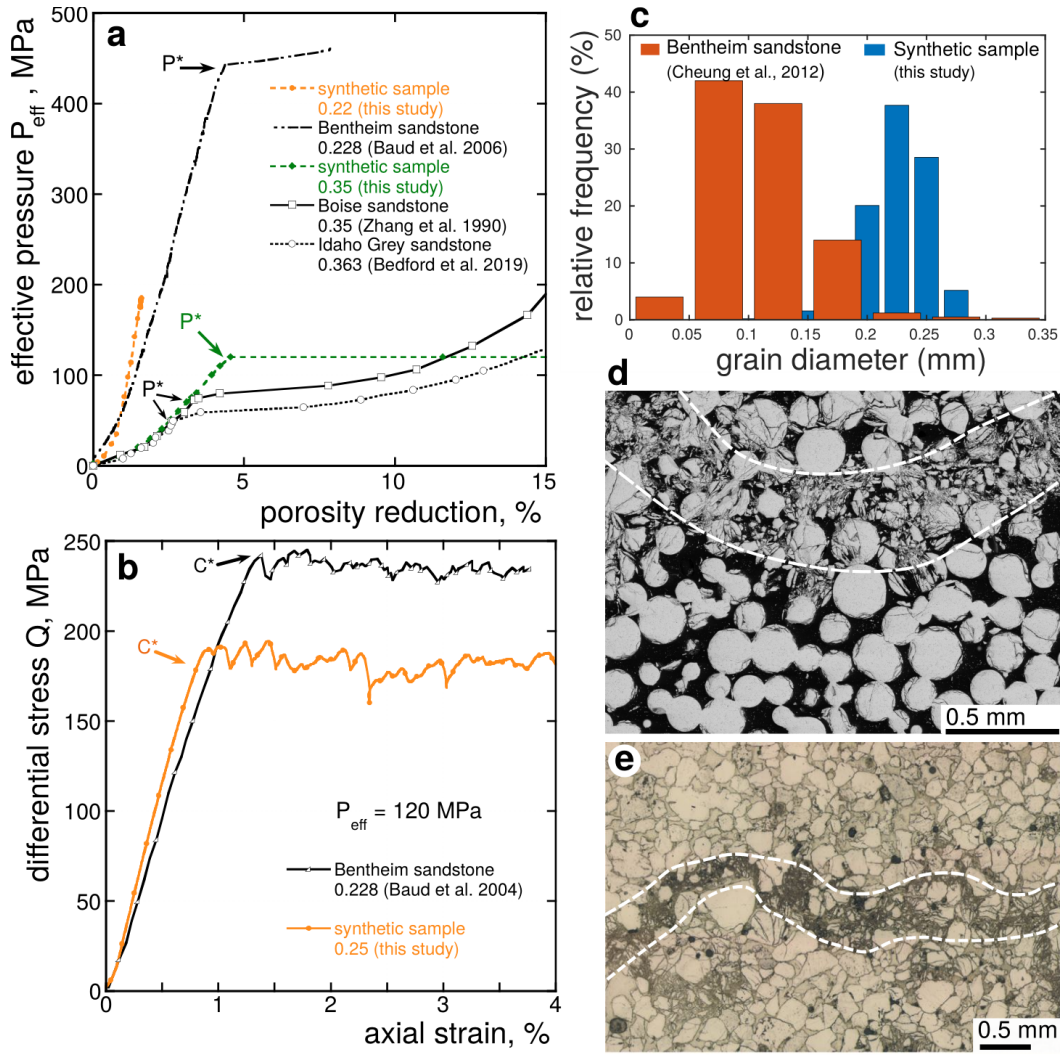


Figure 6 Data from tests performed on synthetic samples compared to data for sandstones from the literature. **(a)** Comparison of the hydrostatic loading curve of a synthetic sample (green dashed) with a porosity of 0.35 and a mean grain diameter of 0.5 mm and of the hydrostatic loading curve of a synthetic sample (orange curve) with a porosity of 0.22 and a mean grain size of 0.2 mm, with the hydrostat of Boise sandstone (black line), with a porosity of 0.35 and a mean grain diameter of 0.92 mm, the hydrostat of Idaho Gray sandstone (dashed black) with a porosity of 0.363 and a mean grain diameter of 0.7 mm and the hydrostat of Bentheim sandstone with a porosity of 0.228 and a grain diameter of 0.3 mm. The onset of grain crushing is indicated as P^* . **(b)** Comparison of stress-strain curves obtained during a triaxial test at an effective pressure of 120 MPa performed on a synthetic sample (orange line) with a porosity of 0.25 and a mean grain diameter of 0.2 mm and on Bentheim sandstone (black line). The onset of shear-enhanced compaction is indicated as C^* . **(c)** For reference, the smallest grain size distribution used in this study is presented along the grain size distribution of Bentheim sandstone. **(d)** Comparison of a scanning electron micrograph of a discrete compaction band observed in a synthetic sample ($\phi = 0.35$) and **(e)** an optical microscope image of a discrete compaction band in Bentheim sandstone ($\phi = 0.23$).

Regarding the hydrostatic behaviour. (Figure 6), it can be noted that, during the initial loading and increase of the effective pressure up to P^* , Boise, Idaho Gray, and the synthetic sample with a porosity of

0.35 present porosity reduction curves that are almost identical. The characteristic “tail” at the beginning of the hydrostat is typically attributed to the closure of microcracks. Assuming the sintered glass beads do not contain microfractures at the beginning of the hydrostatic pressurisation, as indicated from the microstructural analysis of the intact material, the non-linear initial portion of the hydrostat can be attributed to grain rotations and rearrangements, which is corroborated by the positive correlation between the size of the tail (i.e., the amount of compaction) and the porosity of the sample. Qualitatively speaking, the compaction curves evolve differently beyond P^* . While a progressive inflection and strain hardening is observed for both Boise and Idaho Gray sandstones, P^* manifests as a sharp breaking point beyond which the synthetic sample undergoes a porosity reduction of about 0.1 without hardening. For natural porous rocks, the first inflection in the hydrostat corresponds to the inception of grain crushing and increasing the effective pressure beyond this point exacerbates the deformation. The gradual behaviour is absent for the synthetic sample, which experiences extensive grain crushing and porosity loss at the state of stress just higher than P^* . The observation of extensive grain crushing at a stress just above P^* is similar to that reported for Bentheim sandstone, a rock that also contains a closely-clustered monomodal grain size distribution (Figure 6). Examination of the microstructure showed that very few areas in the sample remained uncrushed. Contrary to most natural sandstones, the synthetic rocks are composed of monomodal distributions of uniform grains of identical elastic properties. Thus, the force chains induced in the granular framework during loading are expected to be more homogeneously distributed in the monodisperse synthetic samples. As a result of this homogeneity, when the externally applied effective pressure reaches the critical value P^* , the normal forces induced at the grain contacts must reach the critical value at the same time, and most grains are thus crushed at the same state of stress. Quantitatively, the effective stress at which the onset of grain crushing (P^*) occurs is higher in the synthetic rock (120 MPa) than it is in Boise (75 MPa) and Idaho Gray (55 MPa) sandstones. Several differences between the synthetic and natural samples could be considered to explain the higher P^* in the synthetic samples. First, Boise and Idaho Gray sandstone have a larger average grain diameter. Second, Boise and Idaho Gray sandstone contain minerals other than quartz that are characterised by lower values of fracture toughness, such as feldspar. However, although the mineral composition of the two sandstones is very close, the P^* of Boise sandstone is about 25 MPa higher than that of Idaho Gray sandstone (Figure 6(a)). Therefore, the much higher P^* for the synthetic samples might arise from the difference in grain diameter (the smaller the grains, the stronger the sample).

The behaviour of natural sandstones is also compared with that of synthetic samples under triaxial compression. Figure 6 presents mechanical data from triaxial tests conducted on a synthetic sample with a porosity of 0.3 (orange line) and on Bentheim sandstone (black line) under an effective pressure of 120 MPa. Qualitatively, the stress-strain curves are very similar. Quantitatively, C^* is about 50 MPa higher in Bentheim sandstone than in the synthetic sample and is likely the result of the difference in porosity and grain size (both higher for the synthetic sample). Beyond C^* , the mechanical data for both samples show small stress drops, suggesting that the samples failed by development of compaction localisation.

Overall, the mechanical behaviour of sintered glass beads is very similar to that reported for porous crustal rocks, in particular monodisperse synthetic samples behave, mechanically speaking, similarly to well-sorted monomineralic sandstones such as Bentheim. Together with the results for physical properties such as permeability and wave velocity, measurements of the mechanical properties of the synthetic rocks allowed to demonstrate their suitability as analogues for porous crustal rocks. Building on the results obtained from a systematic analysis of the influence of porosity, mean grain size and grain size distribution

on mechanical behaviour, this thesis provided unprecedented conclusions on the relationship between microstructural attributes and the mechanical behaviour of crustal rocks.

Porosity and grain size control on the mechanical behaviour of crustal rocks

Chapter 3 of the thesis comprises a uniaxial compressive strength (UCS) dataset for monodisperse synthetic samples with four different grain sizes and porosity between 0.06 and 0.33, presented here in Figure 7.

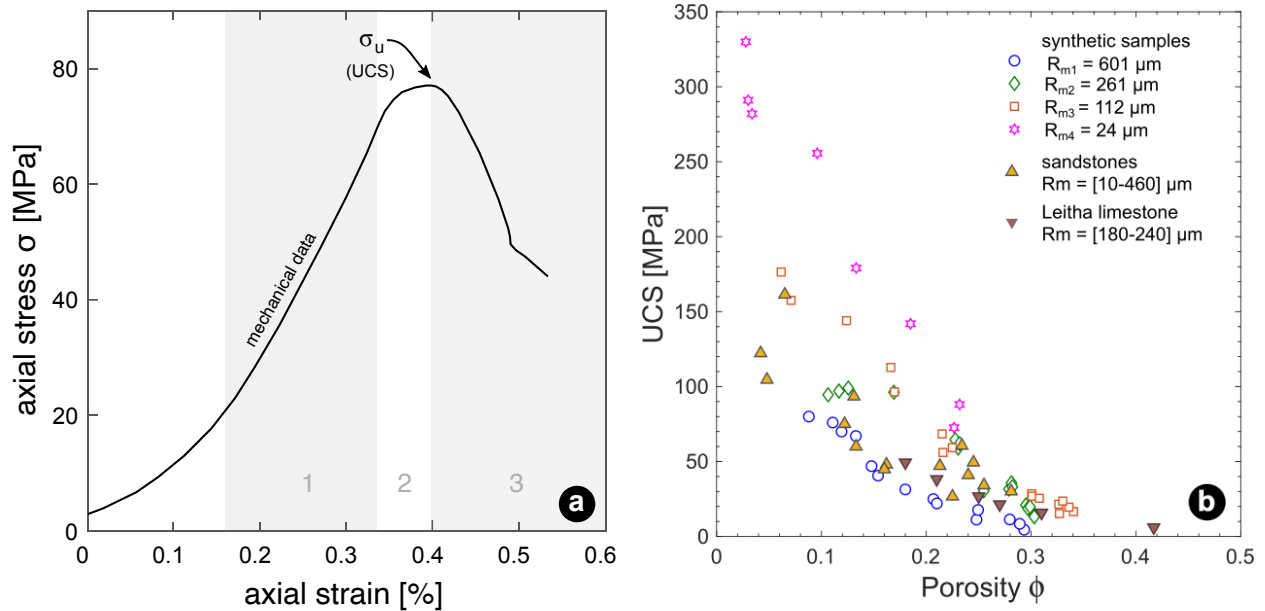
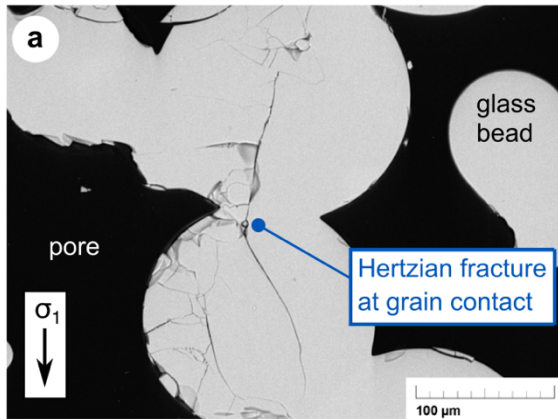


Figure 7 (a) Representative mechanical data for the axial stress change with axial strain during uniaxial deformation. Data presented are for a synthetic sample with $R = 601 \mu m$ and $\phi = 0.11$. The peak stress at brittle failure is marked σ_u . **(b)** Compilation of UCS data for synthetic samples (open symbols) and natural rocks (solid symbols).

In this porosity range, UCS values span a similar range to that reported for fine grained and coarse-grained sandstones. At a given porosity, the higher the mean grain size, the lower the strength. At a given grain size, the strength of synthetic samples decreases almost linearly with porosity. The microstructural data suggest that the mechanism for failure at the grain-scale evolves from pore-emanated cracking in low-porosity samples, which have a non-granular microstructure, to Hertzian cracking in high-porosity samples, which have a granular microstructure (Figure 8).

Herztian cracking at high porosity



Pore-emanated cracking at low porosity

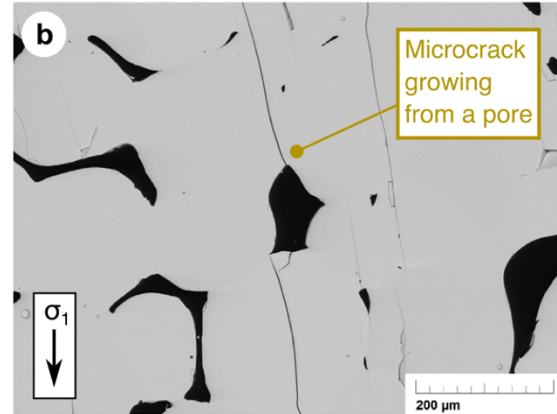


Figure 8 Microstructural deformation features under uniaxial compression. Scanning electron micrographs of samples with a **(a)** high and a **(b)** low porosity deformed up to the peak stress. (a) The microstructure shows that microcracks initiate at grain-to-grain contacts and form Hertzian fractures in poorly sintered samples with a high porosity and a microstructure close to granular. (b) In highly sintered samples, with a low porosity and a microstructure close to non-granular, pore-emanated microcracks grow from the poles of pores.

Such transition might explain the linearity in the porosity-UCS trend in synthetic samples, which has not been reported for natural sandstones but for Leitha limestone, the microstructure of which also transitions from granular to non-granular as porosity decreases by progressive cementation. The threshold porosity for this microstructural transition is positively related to the grain size. Because crustal rocks span the whole range of microstructures between the granular and non-granular endmembers, Chapter 3 demonstrates that sintered glass bead samples can provide hydromechanical results that have applications not only for natural sandstones but also for other granular rocks such as tuffs and some limestones. The uniaxial data presented in Chapter 3 of the thesis have been published in: Carbillet, L., Wadsworth, F. B., Heap, M. J., & Baud, P. (2023). Microstructural controls on the uniaxial compressive strength of porous rocks through the granular to non-granular transition. *Geophysical Research Letters*, 50, e2023GL104678. <https://doi.org/10.1029/2023GL104678>.

Suites of hydrostatic and triaxial deformation experiments were carried out on sintered glass bead samples with porosity of 0.18 - 0.38 and mean grain radius of 112 - 601 μm in order to study the influence of porosity and grain size on the mechanical behaviour and failure mode of porous rocks. The porosity control was investigated while keeping all other microstructural parameters constant (Figure 9).

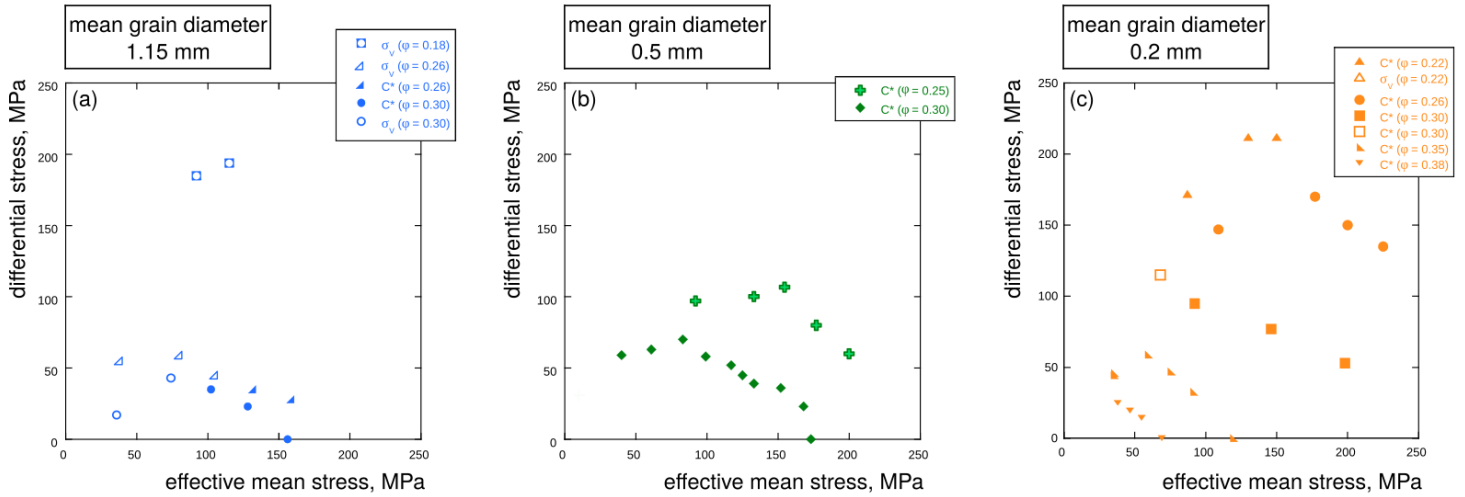


Figure 9 Compilations of failure envelopes for synthetic samples of mean grain diameter of (a) 1.15 mm, (b) 0.5 mm and (c) 0.2 mm. Initial porosity of the synthetic samples is indicated in the legend. Failure envelopes are mapped out by critical stresses σ_v (brittle triaxial test), C^* (ductile triaxial test) and P^* (hydrostatic test). Open symbols correspond to peak stress values and solid symbols to C^* values. P^* (also a solid symbol) anchors the envelope to the x-axis.

Similarly, the influence of the mean grain size of samples with a grain size distribution close to the monodisperse limit was studied while keeping all other microstructural parameters constant (Figure 10).

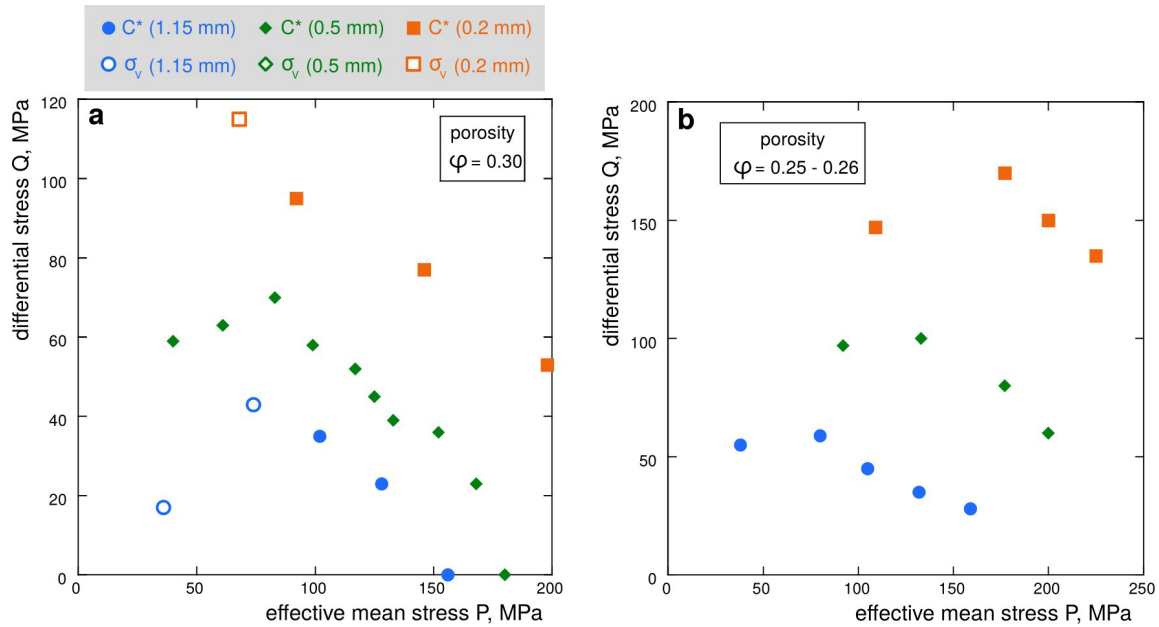


Figure 10 Compilations of failure envelopes for synthetic samples with a porosity of (a) 0.30 and (b) 0.25. Mean grain diameter of the synthetic samples is indicated in the legend. Failure envelopes are mapped out by critical stresses σ_v (brittle triaxial test), C^* (ductile triaxial test) and P^* (hydrostatic test). Open symbols correspond to peak stress values and solid symbols to C^* values. P^* (also a solid symbol) anchors the envelope to the x-axis.

Overall, results showed that, under hydrostatic compression, the onset of grain crushing was reached at a pressure which decreases with increasing porosity or increasing mean grain radius. Under triaxial compression, the brittle-ductile transition occurred at a stress state which decreases with increasing porosity or mean grain radius. The stress for the onset of shear-enhanced compaction is multiplied by two for a decrease in porosity of 0.06 and for a decrease in average grain diameter of 0.50 mm. Such behaviour results in a decrease in the size of the failure envelope with increasing porosity or mean grain radius (Figures 9 and 10). Importantly, results presented in Chapter 4 of the thesis highlight that mean grain size has an influence on the mechanical behaviour as significant as porosity. Therefore, given the broad range of mean grain size that natural porous rocks span, grain radius should systematically be taken into account when studying and modelling the mechanical properties of porous rocks. For example, in the context of depletion-induced reservoir subsidence, measuring the grain size of each reservoir formation will help assess which sedimentary layer will compact first and/or to the highest extent. Indeed, as a decrease of 250 μm in grain radius yields an increase of 50% in the stress to reach inelastic compaction under triaxial compression, coarse-grained reservoir formations can likely undergo compaction earlier and more intensely than fine-grained formations, even if they have very similar porosities.

The influence of grain size distribution on the mechanical behaviour of crustal rocks

In the study of the hydromechanical properties of porous rocks, previous authors pointed out the need for considering the influence of the whole grain size distribution rather than mean grain size, which can only partially describe microstructural geometries. This issue was specifically addressed by performing a suite of deformation tests on sintered glass beads prepared with bidisperse and polydisperse grain size distributions. Figure 11 presents two compilations of mechanical data from hydrostatic and triaxial compression experiments performed on synthetic samples with variably polydisperse grain size distributions, as indicated by the parameter S ($0 < S < 1$, the monodisperse limit).

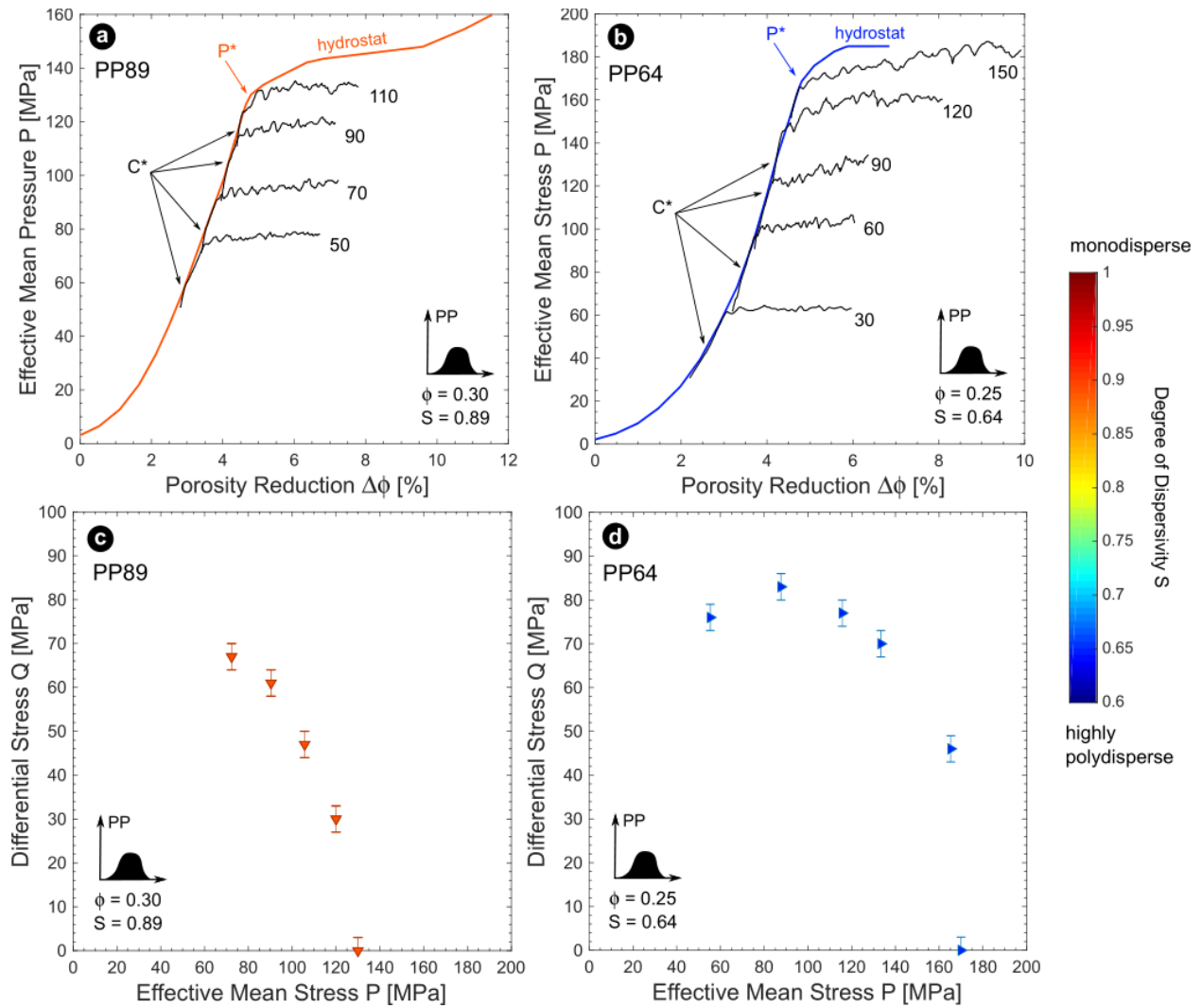


Figure 11 Hydrostatic and triaxial mechanical data for polydisperse (PP) synthetic samples. The effective mean stress-porosity reduction curves for triaxial tests (black lines) are compiled with the corresponding hydrostatic curve (coloured lines) for samples with a grain size distribution PP89 (a) and PP64 (b). The critical stress values (C^* and P^*) are plotted in the P - Q stress space where they map out the compactive yield caps for the distributions (c) PP89 and (d) PP64. The porosity and degree of polydispersity of the samples is indicated in the corner of each corresponding subplot.

The results obtained are presented in Chapter 5 of the thesis. Overall, they showed that an increase in polydispersity decreases the stress and pressure required for the onset of inelastic compaction under triaxial and hydrostatic compression, respectively (Figure 12).

Under hydrostatic compression, the lower critical stress values found for bidisperse and polydisperse synthetic samples are likely due to the homogeneity of the monodisperse sample compared to the bidisperse and polydisperse samples. As the shape and elastic properties of all glass beads are the same, most grains in the monodisperse samples are crushed at the same critical state of stress under hydrostatic loading. On the contrary, in the bidisperse and polydisperse samples, normal forces induced at the grain contacts likely reach the critical value at different values of the externally applied effective pressure,

resulting in an earlier and more gradual transition to inelastic deformation for the bulk sample. This can explain some of the differences between the shape of the hydrostatic curves in Figure 12.

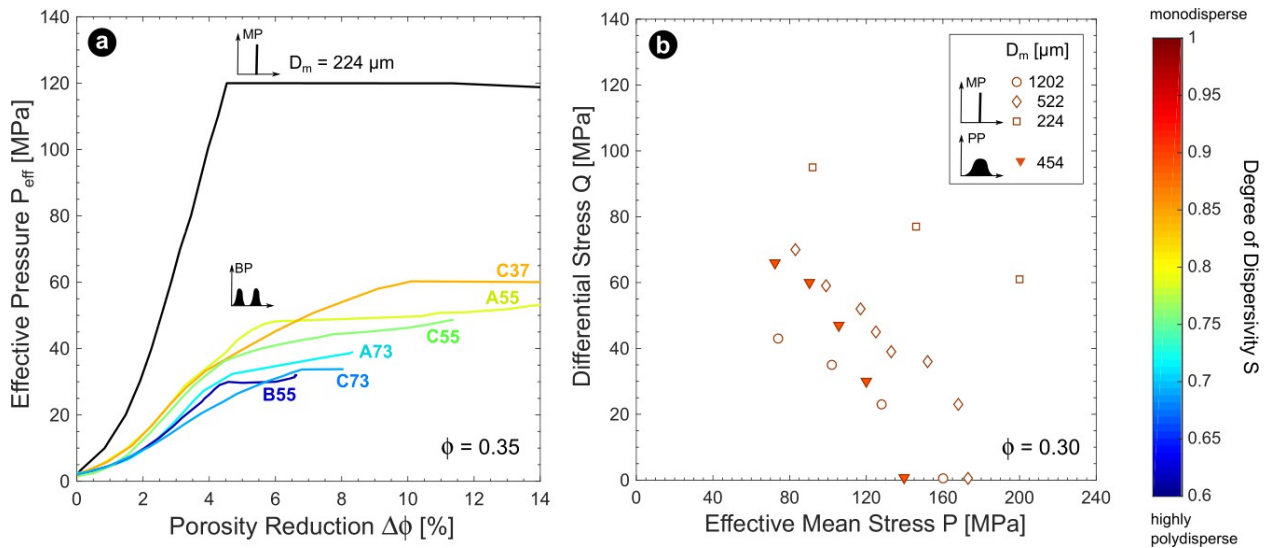


Figure 12 (a) Hydrostatic curves for synthetic samples with a porosity of 0.35 and with bidisperse (BP, coloured curves) and monodisperse (MP, black curve) grain size distributions. **(b)** Compactive yield caps of synthetic samples with a porosity of 0.30 and polydisperse (PP, solid triangles) and monodisperse (open symbols) grain size distributions. The mean of the grain size distributions is given as D_m and the degree of dispersivity S is colour coded using the colour scale on the right.

Under triaxial compression, for a same porosity and similar mean grain diameter, the stresses required to reach C^* are lower for the polydisperse synthetic samples. This is attributed to the fact that the bulk mechanical response of porous rocks is controlled by the arrangement of forces at the grain-scale, that is, by the morphology of the force chain network (defined as the subset of grain-to-grain contacts carrying the largest forces in the system), where straight force chains with a higher degree of branching, which results in a macroscopically stronger granular material, are more likely to form in more polydisperse samples.

In addition, this research also demonstrated that the grain size distribution strongly influences the microstructural deformation features which develop under triaxial compression in the ductile regime. Whilst discrete compaction formed in very well-sorted samples, an increase in dispersivity appears to be accompanied by a progressive transition from localised to delocalised deformation features (Figure 13). Compaction bands were observed down to a degree of dispersivity of 0.65 (where 1 is the monodisperse limit) in synthetic samples, which corresponds to a grain diameter distribution with a minimum of 150 μm and a maximum of 1300 μm , and of 0.70 in natural sandstones. At a degree of dispersivity of 0.53 (Boise sandstone), compaction localisation was inhibited and deformed samples showed delocalized cataclastic flow. Moreover, a change in the modality of the grain size distribution from monomodal to bimodal inhibits compaction localisation, even at a degree of dispersivity of 0.83. Such an observation reveals the importance of the difference between the sizes of the grains, where samples that contain grains with multiple sizes are more likely to undergo compaction localisation than samples that contain grains with only two different sizes.

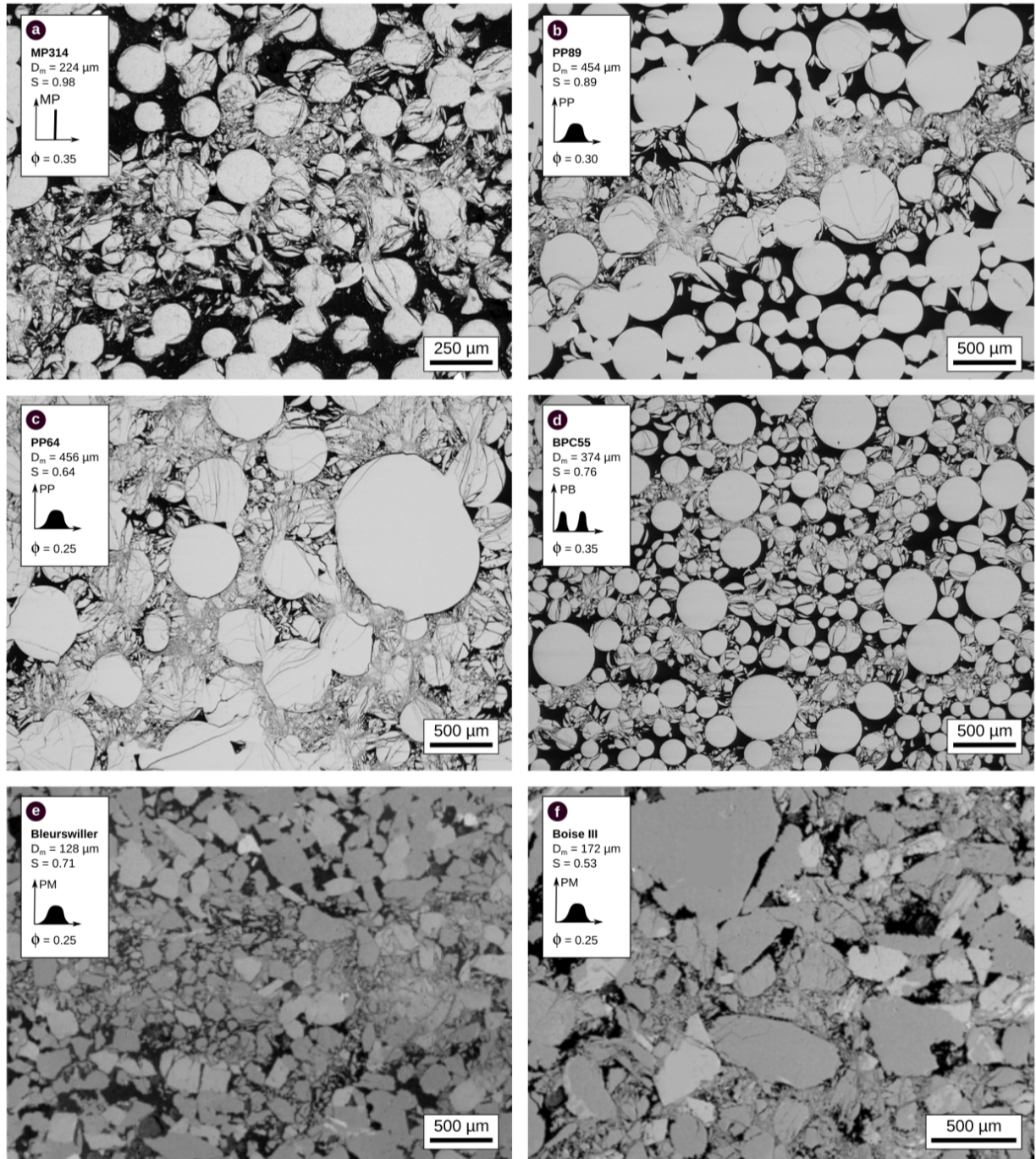


Figure 13 Backscattered scanning electron microscope images of the microstructure of sintered glass bead samples with (a) a monodisperse grain size distribution, (b,c) a polydisperse distribution and (d) a bidisperse distribution compared to that found in Bleurswiller and Boise sandstones, after triaxial testing in the regime of shear-enhanced compaction. The type of distribution, mean grain diameter and degree of polydispersivity of each sample are indicated on the corresponding micrograph.

Overall, the results presented in Chapter 5 of the thesis suggest that there exists a continuous transition from localized to delocalized compaction as the polydispersivity of the grain size distribution

increases. This might be due to the pore space morphology, where local heterogeneities in the pore space, reduced as the width of the grain size distribution increases, act as stress concentrators and promote the growth of compaction bands. Since the synthetic samples are simplified two-phase materials, the grain and pore size distributions are intimately related via pore size functions. For a given mean grain size, broadly speaking, the effect of increasing the width of a grain size distribution is to even further broaden the pore size distribution and to translate it to smaller mean pore sizes, relative to the situation for a monodisperse pore size distribution. This implies that continuously increasing the polydispersity of a system of grains would distribute and tighten the pore spaces relative to a monodisperse system at the same grain size and porosity, which in turn appears to inhibit compaction band formation.

Conclusions and perspectives

The research presented in the thesis *From grains to rocks: the evolution of hydraulic and mechanical properties during diagenesis* provides unprecedented results on the influence of microstructural attributes on the hydromechanical behaviour of porous crustal rocks.

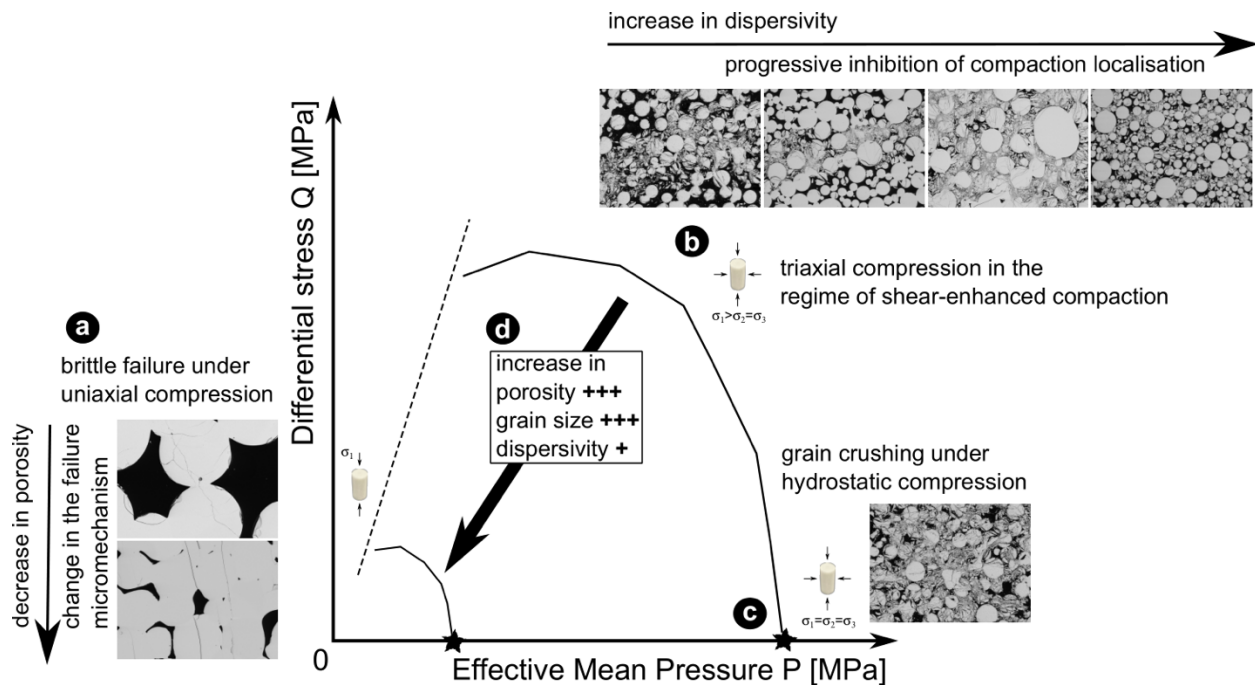


Figure 14 The mechanical behaviour and failure mode of sintered glass bead samples: influence of porosity, grain size and dispersivity of the grain size distribution.

Using synthetic samples which microstructural parameters could be parameterize specifically for the study of porosity, mean grain diameter and the polydispersity of the grain size distribution, it was demonstrated that (Figure 14):

- All else being equal, increasing porosity from 0.22 to 0.35 decreases the stress required to reach inelastic compaction by more than a factor of five.

- All else being equal, increasing mean grain diameter from 0.2 mm to 1.15 mm decreases the stress required to reach inelastic compaction by more than a factor of two.
- An increase in the grain size distribution dispersivity decreases the stress required to reach inelastic compaction under hydrostatic and triaxial compression.
- An increase in the grain size distribution dispersivity results in a transition from localised to delocalisation deformation under triaxial compression.

The use of the viscous sintering of glass beads to prepare synthetic rocks arose largely from the simplicity of the process, the very small number of constituents (which chemico-physical properties are very well constrained), and the broad textural similarities in relation to porous crustal rocks (Chapter 2). Furthermore, this method offers the possibility to deconvolve the porosity and the grain size distribution over a broad range of values: the porosities that can be achieved for a given grain size distribution are comprised between the initial packing porosity (approximately 0.4) and 0.06-0.10 and the grain size distribution can be designed in the limit of the sizes of glass beads which can be purchased or sieved in the laboratory (while adapting the bulk dimensions of the samples to allow for viscous sintering, Chapter 2). Overall, the use of viscous sintering has allowed for the preparation of identical samples, so that tests could be repeated, but also of suites of samples for which only one microstructural attribute was varied while others were kept constant, so that its isolated influence could be explored. Further, over the range of porosity and grain size investigated, it was demonstrated that the sintered glass bead samples have the potential to accurately simulate the evolution of the hydraulic and mechanical properties of natural rocks. However, technical difficulties arise progressively when trying to model more complex microstructures than that of monomineralic well-sorted sandstones, even when the synthetic samples only contain one component and no cement (Chapter 2). In the course of this work, more than 400 samples were prepared and more than 200 deformation experiments were performed, the results of which helped to draw predictive conclusions for porous crustal rocks. However, one might wonder whether a thorough study of the same properties using natural rocks could have provided more extensive insights on their hydromechanical behaviour because it would not have been slowed down by any technical difficulty associated to the manufacturing of synthetic rocks. More simply, one might ask whether using synthetic samples is worth it. Such questioning is resolved by considering that the conclusions that can be drawn using synthetic rocks or using natural rocks can never be the same. As an illustration of this, extrapolating the conclusions drawn using synthetic rocks to natural rocks can be difficult as the behaviour of natural rocks results from the complex coupling between various parameters. Further, while working on natural rocks will allow us to progressively establish an extensive catalogue of the different types of behaviour and tend toward more universal descriptions of the control of specific attributes, synthetic rocks have the potential to provide more definitive and therefore predictive conclusions valid for most porous rocks. As an illustration of this, the work conducted for this thesis provided information about the influence of grain size and grain size distribution that were not known before. Finally, because studies on synthetic or natural rocks can help understanding different aspects of the mechanical behaviour, works on synthetic and natural rocks should be extended collaboratively as far as possible. Indeed, the cohesive integration of laboratory experiments using synthetic and natural rocks, numerical simulations and field observations can serve to further the understanding of the link between the grain scale, the sample scale and the field scale. A particularly interesting way forward would be to develop the comparison between DEM simulations and sintered glass bead samples, where these synthetic rocks should help to set the model parameters and therefore help to move towards more realistic 3D simulations. [Word count: 5903 words]